J. Am. Chem. Soc.

Zero-overlap Fluorophores for Fluorescent Studies at Any Concentration

Ayan Dhara, Tumpa Sadhukhan, Edward G. Sheetz, Andrew H. Olsson, Krishnan Raghavachari and Amar H. Flood*

Department of Chemistry, Indiana University, 800 East Kirkwood Avenue, Bloomington, IN 47405, USA.

ABSTRACT

Fluorophores are powerful tools for the study of chemistry, biology and physics. However, fluorescence is severely impaired when concentrations climb above 5 μM as a result of effects like self-absorption and chromatic shifts in the emitted light. Herein, we report the creation of a charge-transfer (CT) fluorophore and the discovery that its emission color seen at low concentrations is unchanged even at 5 mM, some three orders of magnitude beyond typical limits. The fluorophore is composed of a triphenylamine-substituted cyanostar macrocycle, and it exhibits a remarkable Stokes shift of 15,000 cm^{-1} to generate emission at 633 nm. Crucial to the performance of this fluorophore is observation that its emission spectrum shows near-zero overlap with the absorption band at 325 nm. We propose that reducing the spectral overlap to zero is a key to achieving full fluorescence across all concentrations. The triphenylamine donor and five cyanostilbene acceptor units of the macrocycle generate an emissive CT state. Unlike closely related donor-acceptor control compounds showing dual emission, the cyanostar framework inhibited emission from the second state to create a zero-overlap fluorophore. We demonstrated use of emission spectroscopy for characterization of host-guest complexation at millimolar concentrations, which are typically the exclusive domain of NMR spectroscopy. The binding of the PF_6^- anion generates a 2:1 sandwich complex with blue-shifted emission. Distinct from twisted intramolecular charge-transfer (TICT) states, experiment-supported density functional theory shows a 67º twist inside an acceptor unit in the CT state instead of between the donor and acceptor; it is TICT-like. Inspired by the findings we uncovered similar concentration-independent behavior from a control compound strongly suggesting this behavior may be latent to other large Stokes-shift fluorophores. We discuss strategies capable of generating zero-overlap fluorophores to enable accurate fluorescence characterization of processes across all practical concentrations.

INTRODUCTION

Light-emitting fluorophores are essential to applications in lasing,[1] solar concentrators,[2] bio-imaging,[3-4] biomedical applications,[5,6] and information coding[7-8] as well as fundamental studies in photochemistry[9-11] and supramolecular chemistry.[12-15] However, every quantitative use of fluorescence has the same practical limitation that it must be performed at micromolar (μM) concentrations.[13, 16-17] This limit arises largely from an overlap between the absorption and emission spectra historically characterized by energy differences between absorption and emission maxima, so-called Stokes shift.[18] For example, rhodamine 3B perchlorate has a small Stokes shift of 710 cm^{-1} (Figure 1a). Nevertheless, we see a large spectral overlap (red) responsible for self-quenching by reabsorption of the emitted light[19] and red-shifted emission, known as a secondary inner filter effect.[20] Increasing Stokes shifts has been proposed as a solution to these problems.[21] Some structural characteristics that confer large Stokes shifts are nonsymmetric structures,[22] excited-state proton transfer,[23-24] exciplexes,[25] and charge transfer (CT).[26-28] Large Stokes shifts exceeding 8,000 cm^{-1} for organic[27, 29-32] and inorganic[33-35] fluorophores have been seen. Use of Förster resonance energy transfer (FRET) is another approach.[36] However, residual overlaps remain problematic[32] inhibiting use of fluorophores for studying concentration-driven processes, like supramolecular polymerization,[37] self-reporting polymer micelles,[38] imaging,[39-40] information processing,[41] sensing,[42] and solar concentrators.[43-44] Other problems stemming from aggregate[45-47] or excimer[48-51] formation also produce emission spectra that change with concentration. Thus, there is a critical need for new strategies to address these challenges. We report the discovery of a fluorescent CT macrocycle composed of a triphenylamine (TPA)-substituted cyanostar, called cyanozero (**C-Zero**, Figure 1b), that solves these problems and leads to new strategies for achieving high-concentration fluorescence by creating zero-overlap fluorophores.

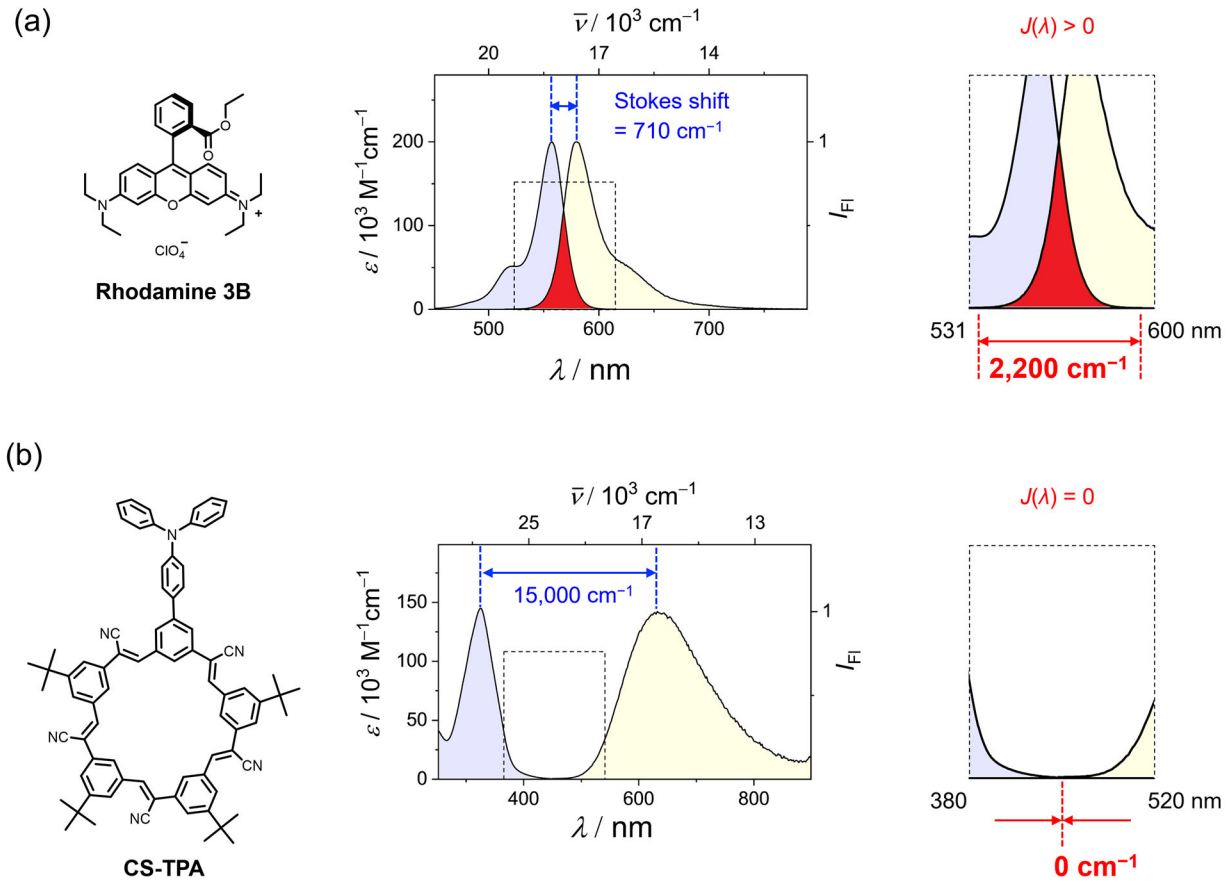

Figure 1. Absorption and emission bands in dichloromethane of (a) traditional fluorophores like rhodamine 3B perchlorate with small Stokes shift and large band overlap. (b) Novel cyanostar-triphenylamine (TPA) fluorophore, called cyanozero (**C-Zero**) with a massive Stokes shift and zero overlap (dichloromethane). Red region highlights overlap between absorption and emission bands. $J(\lambda)$ is the spectral overlap integral.

Large Stokes-shift compounds are a good first step to creating zero-overlap fluorophores. Donor-acceptor compounds are exemplary. One problem, however, is that some of them can show dual emission upon photoexcitation. This behavior is often assigned to a twisted intramolecular charge-transfer (TICT)[31, 52-53] state and its variants.[32] For example, Ma and co-workers[27] para-linked a TPA donor to an α-cyanostilbene acceptor (***p*-aryl-TPA**, Figure 2) that displays a long

wavelength intramolecular CT emission at a phenomenal Stokes shift of 9,700 cm^{-1}. However, it also showed dual emission involving a second state, typically called the locally excited (LE) state emitting at a shorter wavelength to define a smaller Stokes shift of 3,900 cm^{-1}. The dependence of the relative intensities of dual emission from the local and CT states on temperature, solvent polarity and excitation wavelength offers some chance for control.[52-54] Nevertheless, overlap from LE state often remains and strategies to generate zero-overlap fluorophores are outstanding.

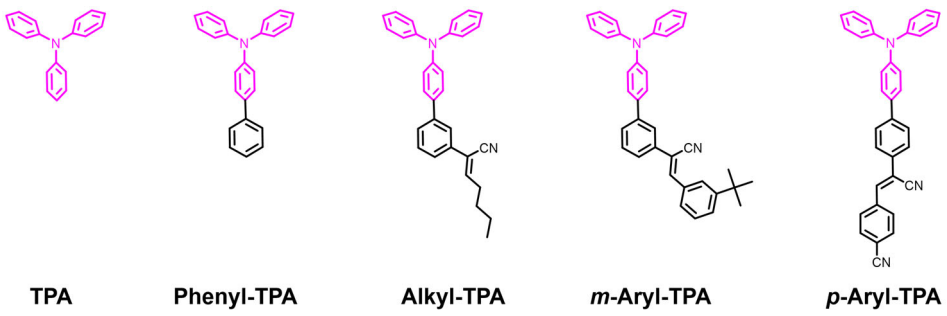

Figure 2. Dual-emission control compounds

The residual spectral overlap (Figure 1, red region) can be defined in a few ways. One way is to use the spectral overlap integral used in the calculation of FRET efficiencies, $J(\lambda)$.[55] The overlap region can also be defined by the difference in energy between the tail ends of the absorption and emission bands when they drop to zero intensity; for rhodamine 3B it extends from 531 to 600 nm. We wish to consider ways to eliminate this 69-nm overlap to enable the monitoring of chemical, biological and physical processes at any concentration of interest.

Towards applications of fluorescence in supramolecular chemistry, use of macrocyclic receptors are ideal. They often have strong binding properties, which can be leveraged for sensing applications[56-57] and for creation of hierarchical assemblies like supramolecular polymers,[58] and interlocked molecules.[59] A common strategy to introduce emission involves attachment of a

fluorophore, e.g., BODIPY[60-61] or naphthalene monoamide.[60] Yet the spectral overlap remains and with it limitations for use at lower concentrations. Strategies to monitor molecular recognition by fluorescence at high concentrations remain outstanding.

We report the serendipitous discovery of a zero-overlap fluorophore in the form of a macrocycle, **C-Zero** (Figure 1b), which is a perfect candidate for the fluorescence monitoring of molecular assembly at any concentration. Our interest is driven by the need to complement the structural information acquired by NMR spectroscopy with fluorescence at the high concentrations needed to form host-guest complexes neatly at their equivalence points. To this end, we faithfully follow host-guest binding[59] at a previously inaccessible concentration using fluorescence spectroscopy for the first time since the inception of supramolecular chemistry over 50 years ago.[62-63] **C-Zero** is based on the anion-binding cyanostar[59] that is monosubstituted by the well-known triphenylamine donor moiety to produce emission from a CT state. We describe the creation of **C-Zero** after the opportune emergence of visible emission seen during synthetic elaboration of the macrocycle. We provide the key test of zero spectral overlap by showing that the emission wavelength (633 nm) does not change with the concentration of the macrocycle from 5 μM up to its solubility limit of 6 mM. The optical properties of control compounds (Figure 2), despite their dual emission, helped understand the origin of the emission properties. Remarkably, emission from the LE state is completely absent in **C-Zero**,[64] which effectively removes all spectral overlap. Our findings show that elimination of local emission from this fluorophore is a viable strategy for the design of zero-overlap fluorophores. The absence of aggregation phenomena is also key to producing this behavior. Looking beyond this result, we show one large Stokes-shift fluorophore that can also be used across concentrations despite its dual emission and believe there may be many more zero-overlap fluorophores in existence.

RESULTS AND DISCUSSIONS

Synthetic Discovery of the Fluorescent Cyanostar Macrocycle. In the course of exploring the post-synthetic modification of cyanostar building blocks (Figure 3a), we discovered that functionalization with amine groups produces visible fluorescence (Figure 3b). Starting with the mono iodo-substituted cyanostar (**CS-I**),[65] cross coupling with the corresponding boronic acid under Suzuki-Miyauara conditions[66] generated the Boc-protected amino-derivative **CS-NHBoc** and the emergence of a sky-blue emission color using UV illumination. Acidic deprotection of the Boc-group yielded the amino-substituted cyanostar **CS-NH_2** and a significant change in emission color to chartreuse yellow. No prior examples of substituted cyanostars had displayed the turn-on of visible emission, which includes macrocycles substituted with either phenyl[67] or π-extended ethynylphenyl groups.[65] We reasoned, therefore, that the emission originated from the introduction of the amino group and was associated with its electron donor properties. Motivated by this rationale, we functionalized the iodocyanostar with a well-known[68] strong triphenylamine donor to make **C-Zero**. The usual Suzuki cross-coupling between monoboronic acid derivative of triphenylamine and **CS-I** provided cyanostar **C-Zero**, which was fully characterized by ^{1}H (Figure 3c) and ^{13}C NMR spectroscopy, and by high resolution electrospray ionization mass spectrometry.

Solutions of each amino-substituted macrocycles are colorless (Figure 3b) suggesting a sizable Stokes shift to the visible glow seen under UV irradiation. To our surprise, **C-Zero** shows one of the largest Stokes shifts known with 308 nm (15,000 cm^{-1}) between absorption (325 nm) and emission (633 nm, ϕ = 0.04, CH_2Cl_2; Table 1). Such a large Stokes shift is unprecedented when compared with prior reports of extraordinarily large Stokes-shifted fluorophores for either organic[27, 29-32] or inorganic compounds.[33-35] We also observe that **C-Zero** has negligible photobleaching under ambient light (Supporting Information). However, the most unique property

of **C-Zero** is that its absorption and emission bands have zero overlap (Figure 1b), which is a rare feature of fluorophoric compounds. For this reason, we undertook an investigation of the origin of the effect and took the opportunity to demonstrate its use in the characterization of host-guest recognition at concentrations normally considered too high to be accurate.

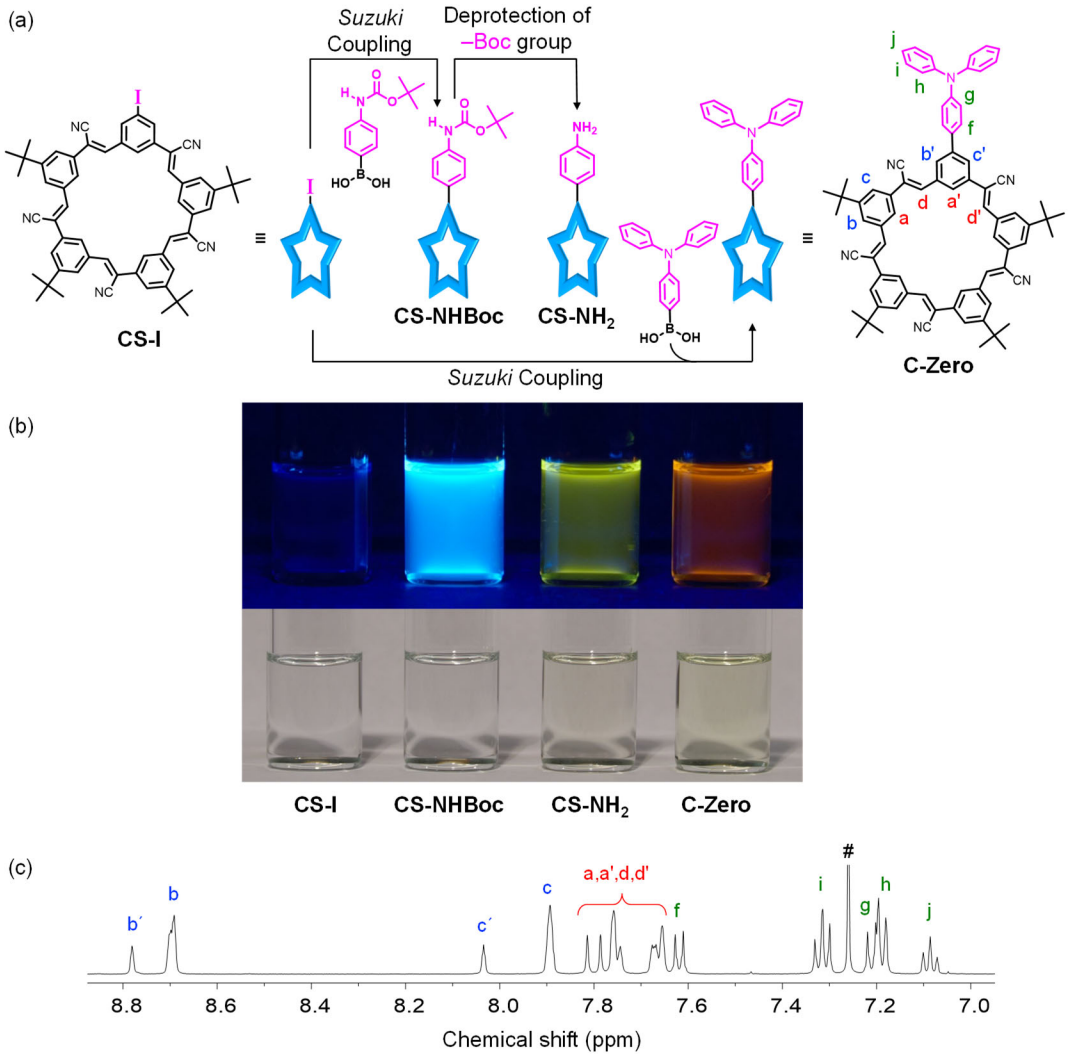

Figure 3. Design evolution and discovery of fluorescent cyanostar macrocycles: (a) Synthesis of **CS-NHBoc**, **CS-NH$_2$**, and **C-Zero**. (b) Solutions of cyanostar derivatives at 5 μM concentrations

in dichloromethane at room temperature under ambient and UV light (λ_{exc} = 365 nm). (c) Partial ^{1}H NMR spectrum of **C-Zero** (0.5 mM / $CDCl_3$ / 600 MHz / 298 K) # = chloroform.

Table 1. Photophysical properties of **C-Zero** (5 μM, CH_2Cl_2)[a]

	$\lambda_{abs,max}$ (nm)	ε (M^{-1} cm^{-1})	$\lambda_{em,max}$ (nm)	Stokes shift (cm^{-1})	τ (μs)	Φ	Brightness
C-Zero	325	145,000	633	15,000	13	0.04	5.8

[a] λ_{exc} = 310 nm for emission and λ_{exc} = 375 nm for lifetime measurement; brightness = extinction coefficient (ε) × fluorescence quantum yield (Φ)[69]

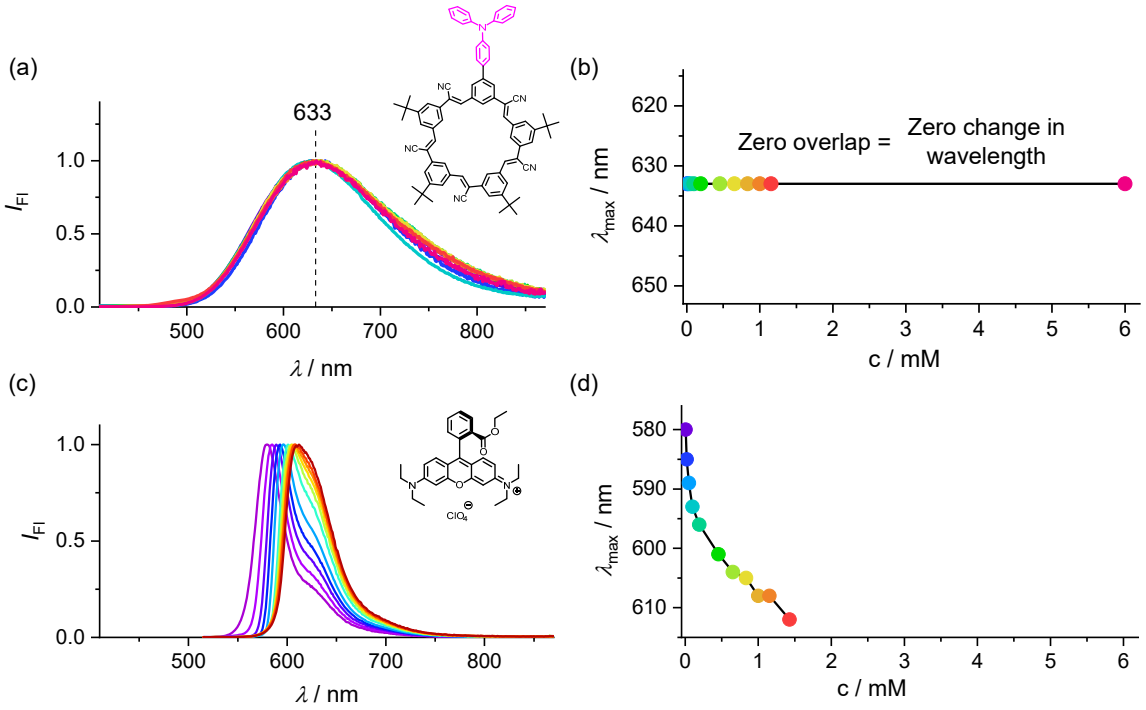

Figure 4. (a) Normalized emission spectra of **C-Zero** (CH_2Cl_2) and (b) emission maxima as a function of concentration (5, 20, 50, 98 and 192 μM, 0.46, 0.65, 0.83, 1.0, 1.2 mM; λ_{exc} = 310 nm). (c) Emission spectra of rhodamine 3B perchlorate (CH_2Cl_2) and (d) emission maxima as a function of concentration (5, 20, 50, 98 and 192 μM, 0.46, 0.65, 0.83, 1.0, 1.2 and 1.4 mM; λ_{exc} = 500 nm.

Compounds with zero overlap between absorption and emission promise no secondary inner filter effects and hence their emission wavelength should be concentration independent.

Despite the simplicity of this idea, and to the best of knowledge, it has not been tested. This idea also requires no aggregation or excimer formation at elevated concentrations. Thus, prior to testing this principle, we verified that this macrocycle did not show any ground-state aggregation from 1 to 222 μM (CH_2Cl_2; Supporting Information) based on the linearity of absorbance.

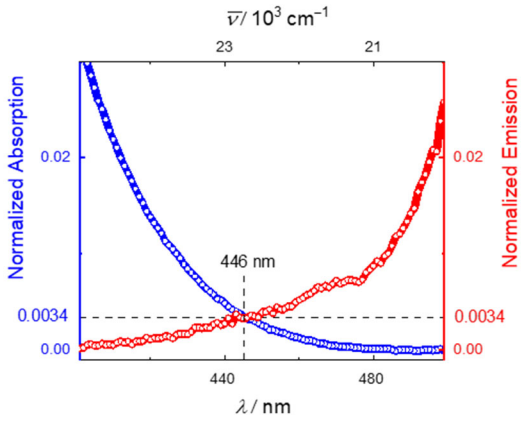

Figure 5. Zoomed-in view of the overlap region between the normalized absorption (blue trace) and emission spectra (red trace) of **C-Zero**.

Consistent with this promise, emission from **C-Zero** does not deviate from 633 nm when examined at low concentrations, such as 5 μM, up to its solubility limit of 6 mM (Figure 4a and b; CH_2Cl_2). We used a 90º sampling geometry for these measurements. As concentration increases, the excitation photons would be absorbed more and more effectively, and would therefore fail to penetrate far into the 1-cm cuvette. However, the emitted light has no overlap with the absorption, and it will therefore pass through the concentrated solution unimpeded by self-absorption. For this reason, we recorded an accurate measure of the emission wavelength as a function of concentration. On the basis of this rationale, there is no need to record the spectra using the front-face geometry favored when recording fluorescence properties at elevated concentrations. Given this preference, however, we repeated the measurement using front-face geometries and confirmed that emission

wavelength is invariant (5 and 192 µM; Supporting Information). This behavior is in sharp contrast to what is generally observed for common fluorophores. For example, the emission band of rhodamine 3B recorded under the same 90º geometry displays a significant 30-nm red shift with increasing concentrations (Figure 4c and 4d).

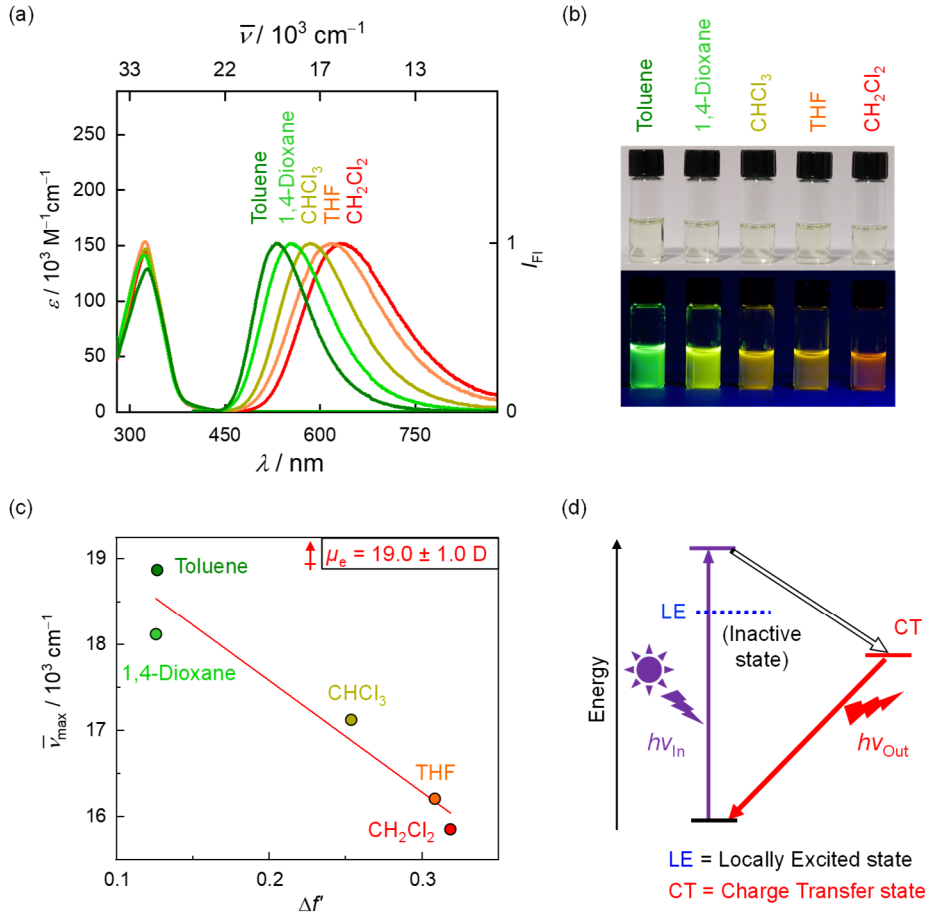

Figure 6. (a) Absorption and emission spectra (λ_{exc} = 310 nm) of **C-Zero** (5 µM) in different solvents. (b) Images of solutions of **C-Zero** (5 µM) in different solvents under ambient and UV light (365 nm). (c) Lippert-Mataga plot of emission energy ($\bar{\nu}_{max}$ / cm^{-1}) for **C-Zero** versus solvent orientation polarizabilities ($\Delta f'$). (d) Proposed model for formation of CT excited state **C-Zero**.

There is a small but negligible degree of spectral overlap for **C-Zero** (Figure 5). The concentration-independent emission wavelength, however, indicates that this overlap is inconsequential up to 5 mM. Thus, we can define an operational limit for generation of zero-overlap fluorophores. At the point of overlap of the normalized absorption and emission spectra of **C-Zero** (446 nm), the absorption and emission spectra reach 0.0034 of their maximum intensities. Rhodamine B perchlorate has substantial overlap (2,200 cm^{-1}) at these same thresholds.

C-Zero Emits from a Charge-transfer Excited State. The 633-nm emission band of **C-Zero** shows no fine structure and does not mirror the absorption band. The absorption band of C-Zero closely matches the parent cyanostar (Figure S7). The full width at half maximum of the emission band is broad (4100 cm^{-1}) relative to rhodamine 3B (900 cm^{-1}). Broad and featureless fluorescence is common to intramolecular CT states[70] or excited-state proton transfer[71] and attributed to high degrees of inhomogeneous line broadening[72] associated with charge redistributions as well as longer lifetimes. Since there is no obvious labile proton, we assume that **C-Zero** emits from an intramolecular CT state. Consistent with this CT character, the fluorescence red-shifts with increasing solvent polarity (Figure 6a and 6b) up to dichloromethane; **C-Zero** has poor solubility in more polar solvents like N,N-dimethylformamide and dimethylsulfoxide, and these solvents were omitted to avoid complications from precipitation. Quantitative analysis of the solvatochromism using the Lippert-Mataga method[73] supports a large 20-Debye dipole in the emissive excited state. We assign this CT state to involving formal oxidation of the **TPA** and formal reduction of the cyanostar (**CS**), thus, [$\mathbf{CS^{-}}$-$\mathbf{TPA^{+}}$]* (Figure 6c). An alternative assignment for the long wavelength emission is excimer formation, which is favored at higher concentrations[74-77] and expected to alter lifetimes. In our tests, however, the emission lifetime of **C-Zero** and is invariant with concentration from 5 mM to 5 mM.

Based on these assessments, and the similarity to the analogous CT fluorophore based on ***p*-aryl-TPA** (Figure 2), we propose an intramolecular CT model (Figure 6d). Another assignment could be derived from a TICT model.[52, 64, 78] To test for the impact of bond twisting on the CT excited state, we measured the emission spectra of **C-Zero** in solvents with similar dielectric constants but different viscosities: toluene ($\varepsilon = 2.4$, $\eta = 0.59$ cP) and 1,4-dioxane ($\varepsilon = 2.2$, $\eta = 1.44$ cP). We observed a decrease in emission intensity with increasing viscosity consistent with the importance of twisting in the excited state. Examples of TICT fluorophores[52-53] and the IUPAC definition prescribe that the donor and acceptor moieties of a molecule are co-planar in the ground state and twisted in the excited state about one of the intervening single bonds to produce orbitally decoupled π-systems. The ground state co-planarity is a less stringent criterion,[79-81] but twisting between donor and acceptor systems appears to be a critical feature.

Computational models suggest the photodriven structural changes of **C-Zero** do not match classical TICT compounds. Geometry-optimized structures obtained using density functional theory (DFT) show donor and acceptor are pre-twisted by 37º in the ground state (Figure 7a). Using time-dependent DFT (TD-DFT), we see that this coordinate does not change upon formation of an excited state. The ground state geometry also shows the macrocycle to be relatively planar, with average torsions of 0º. TD-DFT shows the excited state has one out of the possible five cyano-olefin bonds with substantial twisting (+67º), with the other four close to their near-zero initial torsions (Figure 7). Unlike the IUPAC definition of TICT, there is no change in the bond that separates the donor from acceptor. Instead, only the acceptor moiety undergoes an internal twist. There exist planarized intramolecular charge transfer (PLICT) and planarized and twisted intramolecular charge transfer (PLATICT) fluorophores,[32] which can be obtained based on different combinations of twist angles among donors and acceptors. While the CT characteristics

of **C-Zero** do not fall neatly into any of the boxes, all of the experimental definitions support the influence of intramolecular twisting on the observed CT state of **C-Zero**. Therefore, the best classification of our CT excited states is TICT-like.

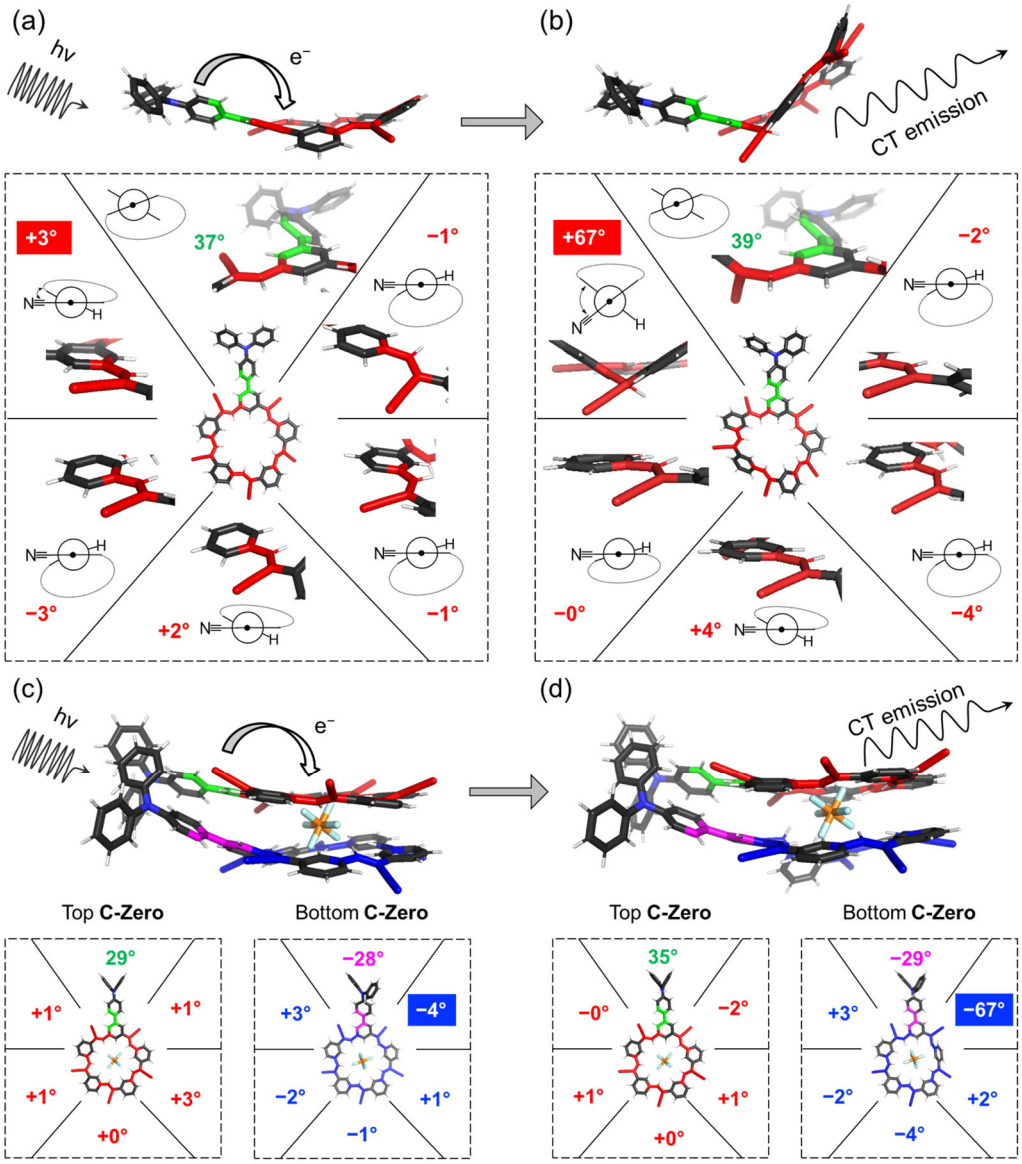

Figure 7. Calculated (a) ground state geometry of **C-Zero** (CAM-B3LYP/6-31+G(d) using a CPCM solvation model for CH_2Cl_2) and (b) CT excited-state geometry using TD-DFT (TD-CAM-B3LYP/6-31+G(d), CPCM solvation model for CH_2Cl_2). Corresponding calculations for the ground-state (c) and excited-state geometries (d) of 2:1 sandwich complex.

Furthermore, the emission from **C-Zero** does not appear to follow the conventional[64] characteristics of dual-emission fluorophores. Excitation using shorter and longer wavelengths usually corresponds to preferential emission from the local excitation[82-83] and lower-energy CT bands, respectively. While this wavelength dependence can unmask dual emission, **C-Zero** only shows one band using 300 to 425 nm excitation (Supporting Information). In TICT compounds, those with pre-twisted ground states tend to suppress the LE state; yet this character does not help explain the observations suggesting that the LE state is inactive in **C-Zero** and that it more closely resembles other types of CT fluorophores.[84-86]

It is not immediately obvious why **C-Zero** does not exhibit dual emission from both the LE and CT state as is seen in the control compound ***m*-aryl-TPA** (vide infra). One rationalization is that, even if a LE state is formed, relaxation might be dominated by non-radiative processes, i.e., its lifetime is too short[19] (<< ns). To test this idea, we measured the emission properties of the parent cyanostar. Consistently, while we see emission at 425 nm, its quantum yield is too low to be measured, i.e., <0.0001. This behavior is consistent with the cyanostar macrocycle's unusually high degree of conformational flexibility with over 300 low-energy conformers.[87] While consistent, this behavior fails to explain why emission from this local state is not observed.

A second hypothesis for sole emission from the CT state stems from the presence of five cyanostilbene acceptors that may increase the probability of electron transfer from the triphenylamine to the macrocycle relative to just one acceptor in ***m*-aryl-TPA**. Photo-driven electron transfer from a donor to multiple acceptors is faster than to just a single acceptor.[88-91] As a consequence, the LE state might never be populated (Figure 6d). Consistently, the TD-DFT reveals a family of CT states close in energy. In either case, the unique properties of this intramolecular CT system appear to stem from the cyanostar.

Emission Spectra of Control Compounds Show Dual Emission. We selected and prepared suitable control compounds to help diagnose the structural origin of the single emission (Figure 6). We used **TPA**, **phenyl-TPA**, **alkyl-TPA** and ***m*-aryl-TPA** on account of the fact that they represent donor-acceptor fragments of **C-Zero**. The ***m*-aryl-TPA** is a *meta*-substituted isomer of the *para*-substituted dual-emission compound studied previously for its mechanochromic properties in the solid state.[27] Compounds **TPA** and **phenyl-TPA** show two emission peaks when excited at appropriate excitation wavelengths (Supporting Information). Based on TD-DFT studies, the longer wavelength emission is assigned to a triplet state consistent with an earlier report.[92]

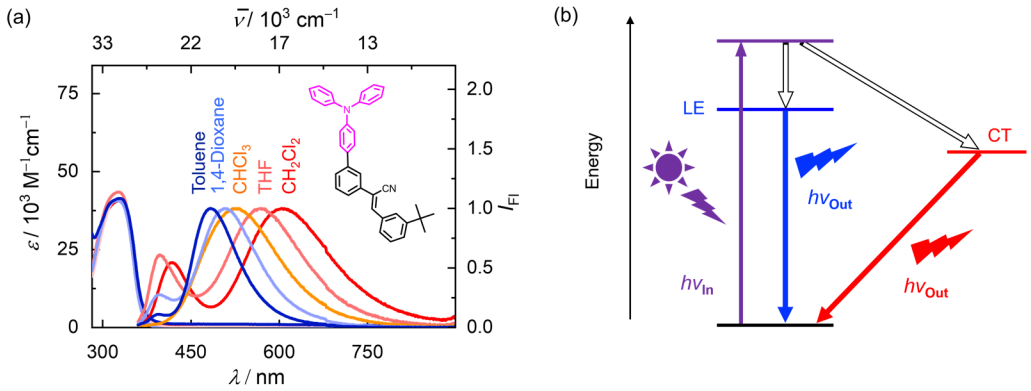

Figure 8. (a) Absorption and emission spectra of ***m*-aryl-TPA** (5 μM, room temperature, λ_{ex} = 340 nm) in different solvents. (b) Assumed energy-state model for the control compounds.

The optical spectra of ***m*-aryl-TPA** are solvent-dependent and the compound shows dual emission (Figure 8). Solvatochromism of the CT band indicate an excited state dipole moment of 14.5 ± 1.5 D. Excimer emission was excluded on the basis of the unchanged lifetime (~13 ns) from 5 μM to 5 mM (CH_2Cl_2). Variable-concentration absorption spectra of ***m*-aryl-TPA** showed a linear response of absorbance with increasing concentrations (50 μM to 5 mM), which suggests no self-aggregation in the ground state (Supporting Information). We also see that this control compound has a large Stokes shift (14,100 cm^{-1}, CH_2Cl_2) similar to **C-Zero**. This result indicates

that a single cyanostilbene is all that is needed for the large Stokes shift. This finding is consistent with the twisting of just a single cyano-olefin seen in the geometry of the CT state of **C-Zero** (Figure 7). TD-DFT on ***m*-aryl-TPA** also shows this bond is twisted albeit to a greater degree, 92º, in the CT state and that it displays two emissive states. Once again, we return to the finding that the absence of the LE state in **C-Zero** requires the macrocyclic framework.

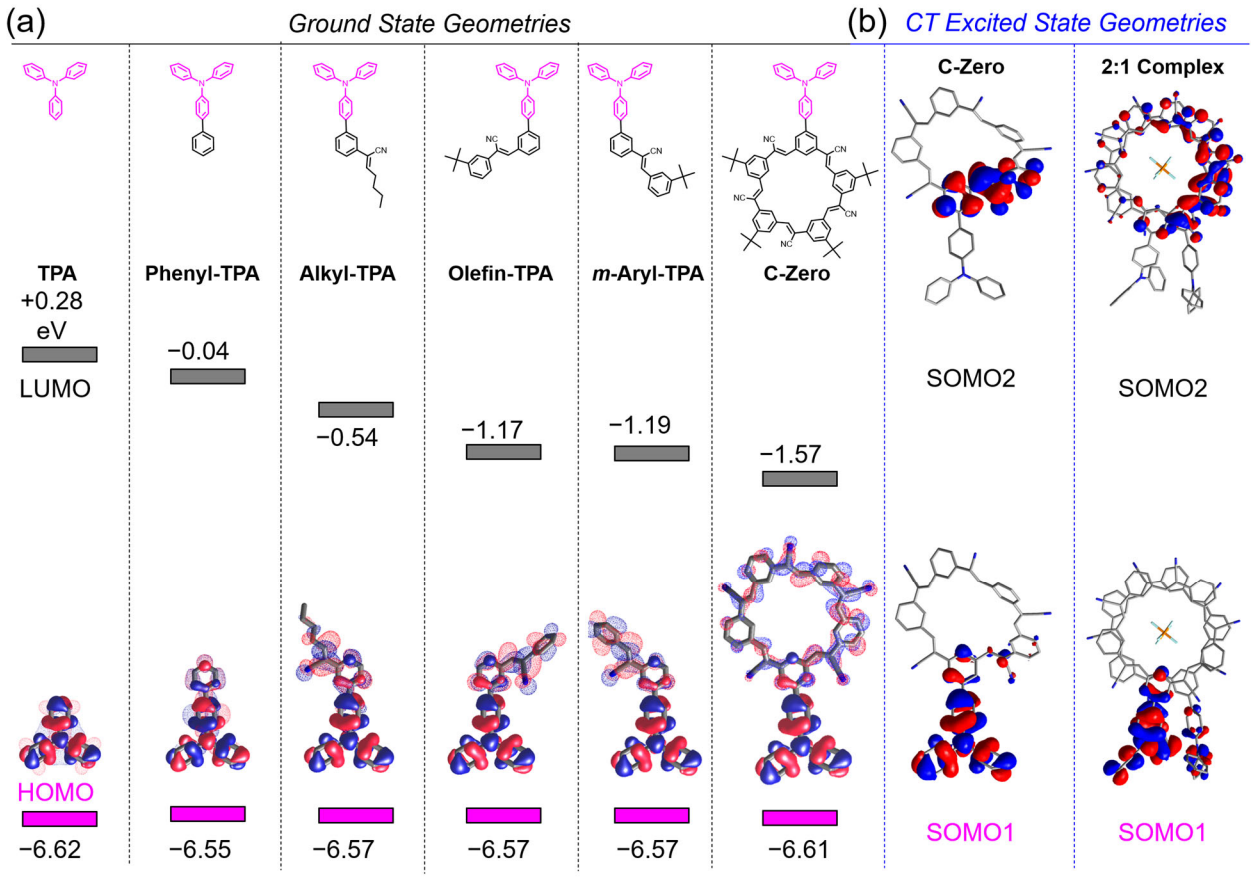

Figure 9. (a) Calculated HOMO (solid) and LUMO (mesh) surfaces of fluorophores and their energy levels (CAM-B3LYP/6-31+G(d) using a CPCM solvation model for CH_2Cl_2). (b) SOMOs for the CT states of **C-Zero** and 2:1 complex computed using TD-DFT.

Electronic Characterization of the Charge-transfer State. Compounds with CT excited states, forming as a consequence of photoinduced electron transfer, are often compared[93-94] to the one-

electron redox products formed by Faradaic electron transfer of the donor and acceptor components. Here, an analogy is made between the configuration of the excited state [**CS**$^{-}$**-TPA**$^{+}$]* and that of reduced cyanostar, **CS**$^{-}$, and oxidized triphenylamine, **TPA**$^{+}$. The **TPA** oxidation occurs at +1.05 V vs. ferrocene (Fc) oxidation to ferrocenium (Fc^{+}) (Supporting Information). The cyanostar reduction[95] is estimated at −1.94 V vs. Fc/Fc^{+} in CH_2Cl_2. The difference is about ~3.0 V, which is equivalent to 415 nm (~24,000 cm^{-1}). Neither the absorption maximum (325 nm) nor emission maximum (633 nm) of **C-Zero** matches this energy gap. The E_{0-0} value is a parameter commonly used for comparison to the CT energies.[96] This value is defined as midway between absorption and emission bands for mirror-image spectra. When not mirror images, the E_{0-0} value is calculated by the intersection of reduced and normalized optical spectra.[97] Based on this approach, the E_{0-0} of **C-Zero** is 471 nm (2.6 eV), which is closer to the 3.0-V gap between redox processes and consistent with the CT assignment [**CS**$^{-}$**-TPA**$^{+}$]*.

DFT computations (Figure 9) verify our assumption that TPA and cyanostar act as donor and acceptor, respectively. The HOMO is localized on TPA with the LUMO delocalized across the cyanostilbenes. The HOMOs remain unchanged across the control compounds. The LUMOs, however, become increasingly stabilized and extended as the acceptor system is spatially enlarged, culminating in full delocalization around cyanostar. Interestingly, this orbital becomes localized in the CT excited state (Figure 9b), represented here as the second singly occupied molecular orbital (SOMO2). In each member of the family of CT excited states observed by TD-DFT, we see a localized twisting. Each member has the distortion localized at just one of the five different olefin sites around the macrocycle.

Fluorescence Responses of C-Zero to Anion Binding. We investigated how anion recognition at high concentrations changes the emission of **C-Zero**. We expected, and found **C-Zero** to display similar anion-binding properties as cyanostar. Specifically, ^{1}H NMR titration of **C-Zero** (0.5 mM, CD_2Cl_2) with tetra-*n*-butylammonium (TBA^+) PF_6^- shows formation of a 2:1 sandwich complex (Supporting Information).[59] Accurate binding constants were obtained from titrations conducted at low concentrations (1 and 5 μM, CH_2Cl_2) as monitored using UV-Vis spectroscopy and subjected to equilibrium-restricted factor analysis as implemented using Sivvu[98] (Supporting Information). We determined all the binding constants based on the following equilibria:

$$\textbf{C-Zero} + PF_6^- \rightleftharpoons (\textbf{C-Zero})\bullet PF_6 \qquad (K_1)$$

$$2\ \textbf{C-Zero} + PF_6^- \rightleftharpoons (\textbf{C-Zero})_2\bullet PF_6 \qquad (\beta_2)$$

The PF_6^- binding affinities of **C-Zero**, $\log K_1 = 5.6 \pm 0.2$ and $\log \beta_2 = 12 \pm 0.5$ correspond to the parent cyanostar,[59] $\log K_1 = 5.6$ and $\log \beta_2 = 12.5$ recorded in 40% MeOH/CH_2Cl_2.

Formation of a 2:1 sandwich complex has multiple mechanisms for altering the optical properties of **C-Zero**. Addition of anions introduces interactions with the acceptor portions of the macrocycle, drives π-stacking of two cyanostar macrocycles,[58-59, 65, 87, 95, 99-114] and brings two triphenylamine units closer together. Consistently, we observed a visual change in color from orange to yellow upon addition of anion (Figure 10a). We see an 11-nm blue shift in the emission upon addition of 10 equivalents of anion to **C-Zero** (5 μM).

Given that the emission maximum of **C-Zero** does not change with concentration, we have the first opportunity to study the change in emission upon guest complexation at millimolar (mM) concentrations unfettered by distortions in the emission's color. These concentrations are several orders of magnitude above all previously studied systems.[13, 16-17] To better understand the change

in fluorescence of **C-Zero** upon the addition of PF_6^- anion, we correlated the emission response to an ^1H NMR titration at 0.5 mM (Figure 10b). The NMR titration showed the predictable curve shape with saturation at 0.5 eq (Figure 10d). Surprisingly, fluorescence showed a different response (Figure 10c; red trace). Instead it showed a turning point at 0.2 equiv. before settling into a plateau at 5 equiv. of added salt. This is a significant deviation from the typical titration curve.

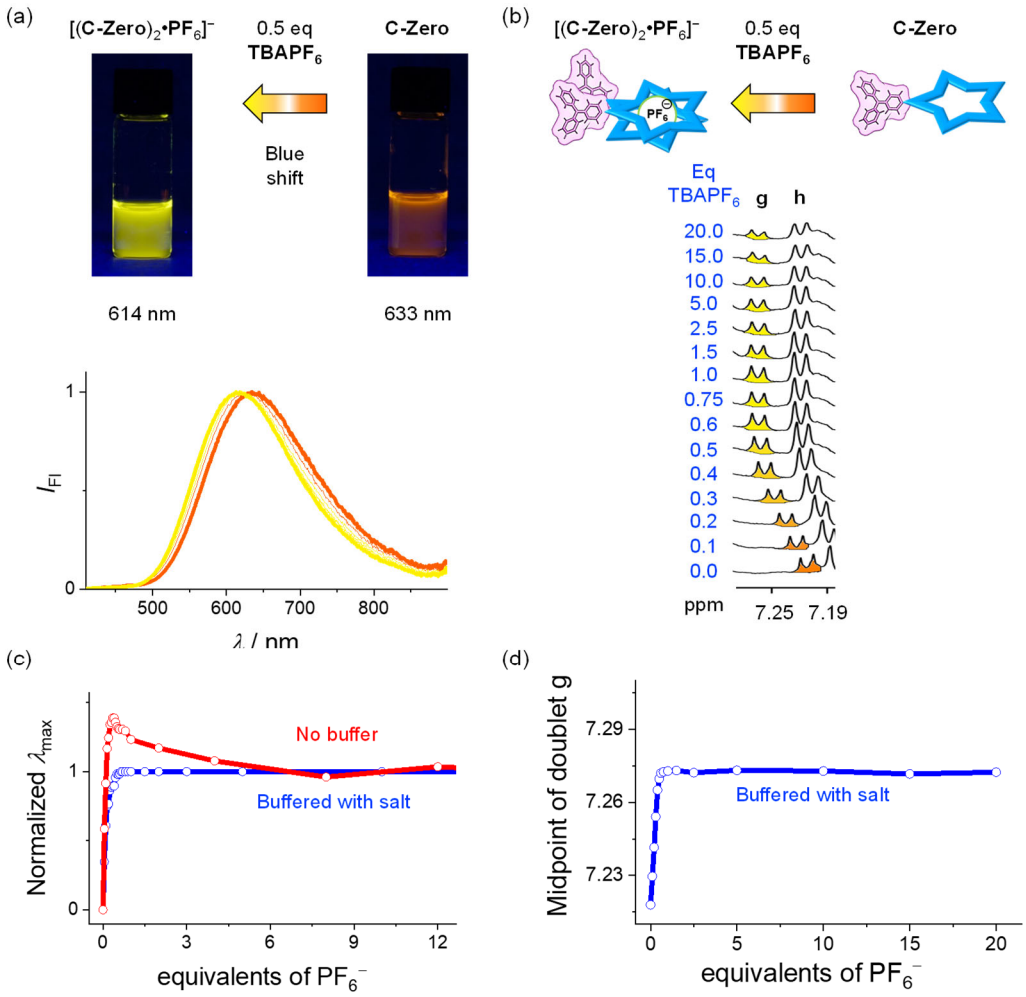

Figure 10. Titration of **C-Zero** (0.5 mM, dichloromethane) with $TBAPF_6$: (a) Emission spectra with 0–0.5 equiv. of $TBAPF_6$. Images show solutions of **C-Zero** with 0.5 equiv. of $TBAPF_6$ under UV-light (365 nm). (b) ^1H-NMR titration buffered with tetrabutylammonium tetraphenylborate

(TBABPh$_4$) salt (25 mM). (c) Titrations showing normalized emission maxima with and without TBABPh$_4$ buffer. (d) Plot of chemical shifts of proton H_g with increasing equivalents of TBAPF$_6$.

Given that fluorescence titrations are never performed at concentrations above ~5 μM, we investigated the possible sources of the deviations in the titration curve. We ultimately attributed this behavior to the high sensitivity of the emissive CT state to its environment, often seen in its solvatochromism (Figure 6). In the titrations, we considered adventitious water and the increases in ionic strength with added salt that lead to changes in solution quality. The ionic strength changes substantially from 1×10^{-5} M to 250×10^{-5} M with 0.2 to 5 equiv. of salt.

An excess of the non-binding anion tetraphenylborate (BPh_4^-) as the TBA^+ salt was added as a spectrochemical buffer[115] to ensure fluorescence is less sensitive to changes in ionic strength and adventitious water. We repeated the NMR (Figure 10b) and emission (Figure 10a) titrations using water-saturated solvents in the presence of an excess of TBABPh$_4$ (50 equivalents; 25 mM). The corresponding ionic strength change is more modest ranging from 25.0×10^{-3} M to 27.5×10^{-3} M with 0–5 equiv. of TBAPF$_6$. The emission maximum wavelength shows the return of a more typical titration curve that now saturates with 0.5 equiv. of added anion (Figure 10c, blue trace). The ^{1}H-NMR titration corroborates this result (Figure 10d) and formation of a high-fidelity 2:1 complex. To the best of our knowledge, this is the first example of fluorophore self-assembly accurately observed by the fluorescence emission spectroscopy at such high concentrations.

It is interesting, however, that the buffered titrations monitored by different spectroscopies generate a small deviation from curves expected for direct formation of the 2:1 species. The fluorescence shows an elevated change in the titration curve's response midway across the 0 – 0.5 equiv. portion. It appears as if these deviations, which dominated in the unbuffered titrations, are

retained to a modest degree even with water saturation and salt buffering. Buffering the ionic strength is an important issue when determining binding constants at high host concentrations. We do not believe this issue had a large impact the measurements we made at low host concentrations (1 – 5 μM). In those cases, ionic strength ([host] = 5 μM) changes from 0 to 0.025×10^{-3} M upon addition of 5 equivalents of $TBAPF_6$. Overall, it appears that water saturation and ionic strength buffering made **C-Zero** fluorescence less sensitive to changes in the solution quality allowing the changes in emission to better reflect the equilibria associated with anion binding.

The blue shift in emission upon formation of the 2:1 complex can be rationalized a number of ways. We undertook calculations to help us understand the shift. DFT calculations indicate the *syn* geometry featuring two contacting TPA moieties is favored by a substantial 7 kcal mol^{-1} (Figure 10b). Analysis of the structure reveals five additional CH•••π interactions between the TPA groups. We note that, despite expectations for enhanced rigidity of the macrocycle in the complex, the extent of bond twisting seen by TD-DFT in the CT state to have the same 67º torsion angle in the single cyano-olefin as seen in the monomolecular species (Figure 7d). Calculations also show a blue shift in the transition energy from 1.7 to 1.6 eV consistent with experiment. Thus, one option is that the PF_6^- anion could destabilize the electron in the acceptor orbital. Alternatively, the *syn* geometry would produce H-type exciton coupling[116] consistent with the blue shift.

Design Strategies for Zero-overlap Fluorophores Interestingly, the reported cyanostilbene fluorophore[27] ***p*-aryl-TPA** might display zero overlap between its absorption and emission spectra in dichloromethane. After digitizing the spectra, we see a small 50 nm overlap (2,050 cm^{-1}) (Figure 11a), which suggests concentration-invariant emission spectra might be possible.

Our findings also raise the opportunity to consider a number of strategies to create zero-overlap fluorophores. First, is to recognize that zero-overlap fluorophores may already exist, such

as ***p*-aryl-TPA**.[27] In the cases that qualify, they need to be tested to show that their emission wavelengths do not change with concentration and then deployed in the study of concentration-driven processes.

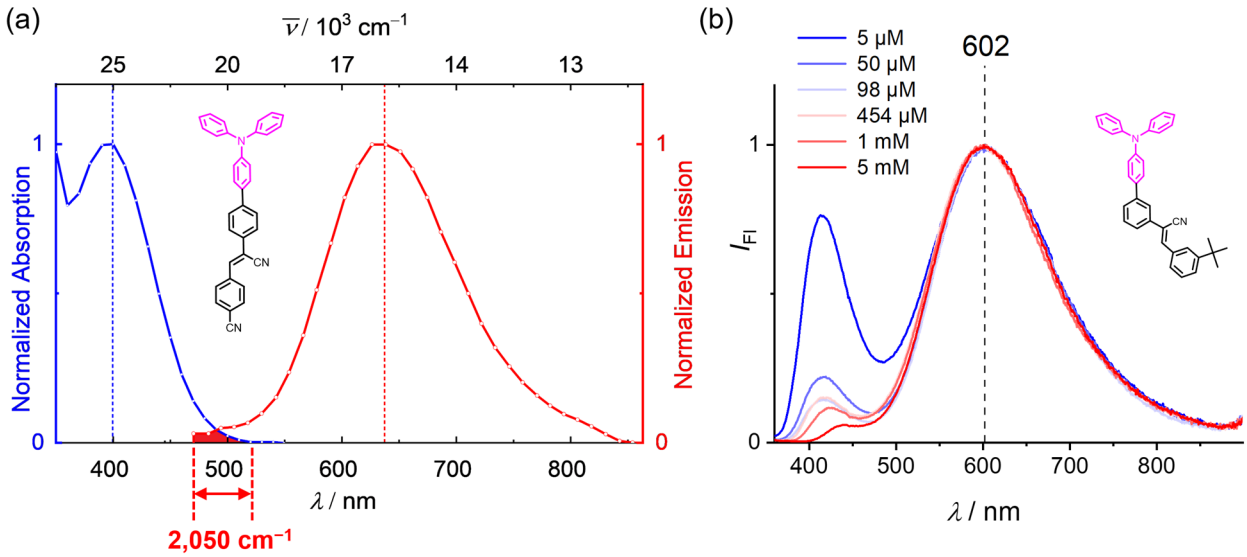

Figure 11. (a) Normalized absorption and emission spectra of ***p*-aryl-TPA** showing the overlap region; data digitized from Ma *et al*.[27] (b) Normalized emission spectra of ***m*-aryl-TPA** recorded as a function of increasing concentration (CH_2Cl_2, λ_{exc} = 340 nm).

A possible example of a latent zero-overlap fluorophore is ***m*-aryl-TPA**. It has a large Stokes shift (Figure 8) to its CT emission but a modest one to the local emission. This example enables us to point a second approach that relies on use of external conditions to extend the Stokes shifts. Use of polar solvents will redshift the CT emission and longer excitation wavelengths are known to disfavor the local emission. In the case of ***m*-aryl-TPA**, use of dichloromethane and 340 nm excitation favors CT emission. However, the LE state and its sizeable 65 nm (4200 cm^{-1}) spectral overlap remain. Nevertheless, we reasoned that while the LE emission would suffer from self-absorption, the CT emission would not. Satisfyingly, the CT emission does not deviate from 602 nm when concentration is raised from 5 μM to 5 mM. Across the same concentration, the LE

peak decreases as expected. This finding suggests that smaller and more modular fluorophores might be useful for broader use in evaluating phenomena at high concentrations.

A third approach, and one realized with **C-Zero**, starts with identifying dual emission fluorophores and leveraging ways to inhibit the local emission. For example, ***p*-aryl-TPA** appears[27] to have the characteristics of a zero-overlap fluorophores in dichloromethane. Other strategies may be accessed by exploiting contemporary ways to increase the Stokes shifts.[22, 24, 26] Finally, use of FRET pairs[117-118] and excimer formation[25, 119] may also prove fruitful.

CONCLUSION

We report on the serendipitous discovery of a fluorescent cyanostar macrocycle with zero overlap between its absorption and emission spectra leading to concentration-independent fluorescence band maxima. We find that the emphasis on obtaining fluorophores with large Stokes shifts is incomplete. Rather, we showcase the benefit of having a fluorophore with zero spectral overlap between its absorption and emission bands. Apart from having a massive Stokes shift (15,000 cm^{-1}), the most important optical property of the **C-Zero** macrocycle appears to be the zero spectral overlap. The key structural characteristic of **C-Zero** is the macrocyclic framework that delivers an intrinsically low quantum yield of local emission and/or enhanced rates of formation of the CT state. Studies on the ***m*-aryl-TPA** control compound verified that having a cyanostilbene-triphenlyamine unit as its core also appears to assist with inhibiting aggregation in good solvents, inhibiting excimer formation, and producing a large Stokes shift from an internally twisted cyanostilbene. The unique characteristics of the **C-Zero** macrocycle enabled us to study anion recognition at millimolar (mM) concentrations for the first time by fluorescence

spectroscopy. We also implemented the concepts governing zero-overlap fluorophores to reveal that the control compound, ***m*-aryl-TPA**, displays some degree of concentration-invariant emission from its CT state. We believe that the creation of zero-overlap fluorophores offers a new, powerful, and complementary approach to observing chemical processes at high concentrations using fluorescence spectroscopy.

ASSOCIATED CONTENT

Supporting Information

The Supporting Information is available free of charge on the journal website.

Experimental procedures, compound characterization, ^{1}H NMR titrations, UV-vis titrations, emission spectra, emission titrations, computational details

AUTHOR INFORMATION

Corresponding Authors

*aflood@indiana.edu

Notes

The authors declare no competing financial interests.

ACKNOWLEDGEMENTS

We acknowledge support from the National Science Foundation (CHE 1709909). We thank Dr. Katherine VanDenburgh for helping us to take the photographs of the fluorescent solutions.

REFERENCES

1. Watanabe, K.; Taniguchi, T.; Kanda, H., Direct-bandgap properties and evidence for ultraviolet lasing of hexagonal boron nitride single crystal. *Nat. Mater.* **2004**, *3*, 404-409.

2. Banal, J. L.; Zhang, B.; Jones, D. J.; Ghiggino, K. P.; Wong, W. W., Emissive Molecular Aggregates and Energy Migration in Luminescent Solar Concentrators. *Acc. Chem. Res.* **2017**, *50*, 49-57.

3. Lavis, L. D.; Raines, R. T., Bright Ideas for Chemical Biology. *ACS Chem. Biol.* **2008**, *3*, 142–155.

4. Xu, W.; Zeng, Z.; Jiang, J. H.; Chang, Y. T.; Yuan, L., Discerning the Chemistry in Individual Organelles with Small-Molecule Fluorescent Probes. *Angew Chem Int Ed Engl* **2016**, *55*, 13658-13699.

5. Ding, F.; Zhan, Y.; Lu, X.; Sun, Y., Recent advances in near-infrared II fluorophores for multifunctional biomedical imaging. *Chem. Sci.* **2018**, *9*, 4370-4380.

6. Wu, X.; Sun, X.; Guo, Z.; Tang, J.; Shen, Y.; James, T. D.; Tian, H.; Zhu, W., In vivo and in situ tracking cancer chemotherapy by highly photostable NIR fluorescent theranostic prodrug. *J. Am. Chem. Soc.* **2014**, *136*, 3579-3588.

7. Wang, H.; Ji, X.; Page, Z. A.; Sessler, J. L., Fluorescent materials-based information storage. *Mater. Chem. Front.* **2020**, *4*, 1024-1039.

8. Yang, Y. D.; Ji, X.; Lu, Z. H.; Yang, J.; Gao, C.; Zhang, H.; Tang, B. Z.; Sessler, J. L.; Gong, H. Y., Time-dependent solid-state molecular motion and colour tuning of host-guest systems by organic solvents. *Nat. Commun.* **2020**, *11*, 77.

9. Cheng, Y. Y.; Khoury, T.; Clady, R. G.; Tayebjee, M. J.; Ekins-Daukes, N. J.; Crossley, M. J.; Schmidt, T. W., On the efficiency limit of triplet-triplet annihilation for photochemical upconversion. *Phys. Chem. Chem. Phys.* **2010**, *12*, 66-71.

10. Gray, V.; Dzebo, D.; Lundin, A.; Alborzpour, J.; Abrahamsson, M.; Albinsson, B.; Moth-Poulsen, K., Photophysical characterization of the 9,10-disubstituted anthracene chromophore and its applications in triplet–triplet annihilation photon upconversion. *J. Mater. Chem. C* **2015**, *3*, 11111-11121.

11. Raisys, S.; Jursenas, S.; Simon, Y. C.; Weder, C.; Kazlauskas, K., Enhancement of triplet-sensitized upconversion in rigid polymers via singlet exciton sink approach. *Chem. Sci.* **2018**, *9*, 6796-6802.

12. Biedermann, F.; Elmalem, E.; Ghosh, I.; Nau, W. M.; Scherman, O. A., Strongly fluorescent, switchable perylene bis(diimide) host-guest complexes with cucurbit[8]uril in water. *Angew. Chem. Int. Ed.* **2012**, *51*, 7739-7743.

13. Yamashina, M.; Sartin, M. M.; Sei, Y.; Akita, M.; Takeuchi, S.; Tahara, T.; Yoshizawa, M., Preparation of Highly Fluorescent Host-Guest Complexes with Tunable Color upon Encapsulation. *J. Am. Chem. Soc.* **2015**, *137*, 9266-9269.

14. Chung, Y. M.; Raman, B.; Kim, D. S.; Ahn, K. H., Fluorescence modulation in anion sensing by introducing intramolecular H-bonding interactions in host-guest adducts. *Chem. Commun.* **2006**, 186-188.

15. Wuerthner, F.; Yao, S.; Beginn, U., Highly ordered merocyanine dye assemblies by supramolecular polymerization and hierarchical self-organization. *Angew. Chem. Int. Ed.* **2003**, *42*, 3247-3250.

16. Duan, H.; Li, Y.; Li, Q.; Wang, P.; Liu, X.; Cheng, L.; Yu, Y.; Cao, L., Host-Guest Recognition and Fluorescence of a Tetraphenylethene-Based Octacationic Cage. *Angew. Chem. Int. Ed.* **2020**, 59, 2-12.

17. Wang, Q.; Zhang, Q.; Zhang, Q. W.; Li, X.; Zhao, C. X.; Xu, T. Y.; Qu, D. H.; Tian, H., Color-tunable single-fluorophore supramolecular system with assembly-encoded emission. *Nat. Commun.* **2020**, *11*, 158.

18. Stokes, G., On the change in Refrangibility of Light. *Philos. Trans. Royal Soc.* **1852**, 463-562.

19. Lakowicz, J., *Principles of Fluorescence Spectroscopy, 3rd ed.* Springer-Verlag: New York: 2006.

20. Tucker, S. A.; Amszi, V. L.; William E. Acree, J., Primary and secondary inner filtering. Effect of $K_2Cr_2O_7$ on fluorescence emission intensities of quinine sulfate. *J. Chem. Educ.* **1992**, 69, A8.

21. Fonin, A. V.; Sulatskaya, A. I.; Kuznetsova, I. M.; Turoverov, K. K., Fluorescence of dyes in solutions with high absorbance. Inner filter effect correction. *PLoS One* **2014**, *9*, e103878.

22. Ren, T. B.; Xu, W.; Zhang, W.; Zhang, X. X.; Wang, Z. Y.; Xiang, Z.; Yuan, L.; Zhang, X. B., A General Method To Increase Stokes Shift by Introducing Alternating Vibronic Structures. *J. Am. Chem. Soc.* **2018**, *140*, 7716-7722.

23. Sedgwick, A. C.; Wu, L.; Han, H. H.; Bull, S. D.; He, X. P.; James, T. D.; Sessler, J. L.; Tang, B. Z.; Tian, H.; Yoon, J., Excited-state intramolecular proton-transfer (ESIPT) based fluorescence sensors and imaging agents. *Chem. Soc. Rev.* **2018**, *47*, 8842-8880.

24. Padalkar, V. S.; Seki, S., Excited-state intramolecular proton-transfer (ESIPT)-inspired solid state emitters. *Chem. Soc. Rev.* **2016**, *45*, 169-202.

25. Chan, K. M.; Kolmel, D. K.; Wang, S.; Kool, E. T., Color-Change Photoswitching of an Alkynylpyrene Excimer Dye. *Angew. Chem. Int. Ed.* **2017**, *56*, 6497-6501.

26. Peng, X. S., F; Lu, E; Wang, Y; Zhou, W; Fan, J; and Gao, Y, Heptamethine Cyanine Dyes with a Large Stokes Shift and Strong Fluorescence: A Paradigm for Excited-State Intramolecular Charge Transfer. *J. Am. Chem. Soc.* **2005**, *127*, 4170-4171.

27. Zhang, Y.; Wang, K.; Zhuang, G.; Xie, Z.; Zhang, C.; Cao, F.; Pan, G.; Chen, H.; Zou, B.; Ma, Y., Multicolored-fluorescence switching of ICT-type organic solids with clear color difference: mechanically controlled excited state. *Chem. Eur. J.* **2015**, *21*, 2474-2479.

28. Shao, B.; Qian, H.; Li, Q.; Aprahamian, I., Structure Property Analysis of the Solution and Solid-State Properties of Bistable Photochromic Hydrazones. *J. Am. Chem. Soc.* **2019**, *141*, 8364-8371.

29. Shcherbakova, D. M.; Hink, M. A.; Joosen, L.; Gadella, T. W.; Verkhusha, V. V., An orange fluorescent protein with a large Stokes shift for single-excitation multicolor FCCS and FRET imaging. *J. Am. Chem. Soc.* **2012**, *134*, 7913-7923.

30. Araneda, J. F.; Piers, W. E.; Heyne, B.; Parvez, M.; McDonald, R., High Stokes shift anilido-pyridine boron difluoride dyes. *Angew. Chem. Int. Ed.* **2011**, *50*, 12214-12217.

31. Liese, D.; Haberhauer, G., Rotations in Excited ICT States - Fluorescence and its Microenvironmental Sensitivity. *Isr. J. Chem.* **2018**, *58*, 813-826.

32. Haberhauer, G., Planarized and Twisted Intramolecular Charge Transfer: A Concept for Fluorophores Showing Two Independent Rotations in Excited State. *Chem. Eur. J.* **2017**, *23*, 9288-9296.

33. Smith, M. D.; Watson, B. L.; Dauskardt, R. H.; Karunadasa, H. I., Broadband Emission with a Massive Stokes Shift from Sulfonium Pb–Br Hybrids. *Chem. Mat.* **2017**, *29*, 7083-7087.

34. Bogh, S. A.; Carro-Temboury, M. R.; Cerretani, C.; Swasey, S. M.; Copp, S. M.; Gwinn, E. G.; Vosch, T., Unusually large Stokes shift for a near-infrared emitting DNA-stabilized silver nanocluster. *Methods Appl. Fluoresc.* **2018**, *6*, 024004.

35. Luo, Y.; Hau, C. K.; Yeung, Y. Y.; Wong, K. L.; Shiu, K. K.; Tanner, P. A., Massive Stokes shift in 12-coordinate Ce(NO2)6(3-): crystal structure, vibrational and electronic spectra. *Sci. Rep.* **2018**, *8*, 16557.

36. Komatsu, T.; Kikuchi, K.; Takakusa, H.; Hanaoka, K.; Ueno, T.; Kamiya, M.; UranoT, Y.; Nagano, e., Design and Synthesis of an Enzyme Activity-Based Labeling Molecule with Fluorescence Spectral Change. *J. Am. Chem. Soc.* **2006**, *128*, 15946-15947.

37. Gao, Z.; Han, Y.; Wang, F., Cooperative supramolecular polymers with anthraceneendoperoxide photo-switching for fluorescent anti-counterfeiting. *Nat. Commun.* **2018**, *9*, 3977.

38. Robin, M. P.; Osborne, S. A.; Pikramenou, Z.; Raymond, J. E.; O'Reilly, R. K., Fluorescent Block Copolymer Micelles That Can Self-Report on Their Assembly and Small Molecule Encapsulation. *Macromolecules* **2016**, *49*, 653-662.

39. Geertsema, H. J.; Schulte, A. C.; Spenkelink, L. M.; McGrath, W. J.; Morrone, S. R.; Sohn, J.; Mangel, W. F.; Robinson, A.; van Oijen, A. M., Single-molecule imaging at high fluorophore concentrations by local activation of dye. *Biophys J* **2015**, *108*, 949-956.

40. Adams, S. R.; Harootunian, A. T.; Buechler, Y. J.; Taylor, S. S.; Tsien, R. Y., Fluorescence ratio imaging of cyclic AMP in single cells. *Nature* **1991**, *349*, 694–697.

41. Raymo, F. M., Digital Processing and Communication with Molecular Switches. *Adv. Mater.* **2002**, *14*, 401-414.

42. Anzenbacher, P., Jr.; Lubal, P.; Bucek, P.; Palacios, M. A.; Kozelkova, M. E., A practical approach to optical cross-reactive sensor arrays. *Chem. Soc. Rev.* **2010**, *39*, 3954-3979.

43. Sark, W. G. J. H. M. v.; Barnham, K. W. J.; Slooff, L. H.; Chatten, A. J.; Büchtemann, A.; Meyer, A.; McCormack, S. J.; Koole, R.; Farrell, D. J.; Bose, R.; Bende, E. E.; Burgers, A. R.; Budel, T.; Quilitz, J.; Kennedy, M.; Meyer, T.; Donegá, C. D. M.; Meijerink, A.; Vanmaekelbergh, D., Luminescent Solar Concentrators - A review of recent results. *Optics Express* **2008**, *16*, 21773-21792.

44. MacQueen, R. W.; Tayebjee, M. J. Y.; Webb, J. E. A.; Falber, A.; Thordarson, P.; Schmidt, T. W., Limitations and design considerations for donor–acceptor systems in luminescent solar concentrators: the effect of coupling-induced red-edge absorption. *Journal of Optics* **2016**, *6*, 064010

45. Hong, Y.; Lam, J. W.; Tang, B. Z., Aggregation-induced emission. *Chem. Soc. Rev.* **2011**, *40*, 5361-5388.

46. Rosch, U.; Yao, S.; Wortmann, R.; Wuerthner, F., Fluorescent H-aggregates of merocyanine dyes. *Angew. Chem. Int. Ed.* **2006**, *45*, 7026-7030.

47. Wuerthner, F.; Saha-Moller, C. R.; Fimmel, B.; Ogi, S.; Leowanawat, P.; Schmidt, D., Perylene Bisimide Dye Assemblies as Archetype Functional Supramolecular Materials. *Chem. Rev.* **2016**, *116*, 962-1052.

48. Foerster, T., Excimers. *Angew. Chem. Int. Ed.* **1969**, *8*, 333–343.

49. Ferreira, J. A.; Porter, G., Concentration Quenching and Excimer Formation by Perylene in Rigid Solutions. *J. Chem. Soc., Faraday Trans. 2* **1977**, 340–348.

50. Birks, J. B.; Christophorou, L. G., Excimer fluorescence spectra of pyrene derivatives. *Spectrochim. Acta* **1963**, *19*, 401.

51. Vollbrecht, J., Excimers in organic electronics. *New J. Chem.* **2018**, *42*, 11249-11254.

52. Grabowski, Z. R.; Rotkiewicz, K., Structural Changes Accompanying Intramolecular Electron Transfer: Focus on Twisted Intramolecular Charge-Transfer States and Structures. *Chem. Rev.* **2003**, *103*, 3899-4032.

53. Sasaki, S.; Drummen, G. P. C.; Konishi, G.-i., Recent advances in twisted intramolecular charge transfer (TICT) fluorescence and related phenomena in materials chemistry. *J. Mater. Chem. C* **2016**, *4*, 2731-2743.

54. Leu, W. C.; Fritz, A. E.; Digianantonio, K. M.; Hartley, C. S., Push-pull macrocycles: donor-acceptor compounds with paired linearly conjugated or cross-conjugated pathways. *J. Org. Chem.* **2012**, *77*, 2285-2298.

55. Verhoeven, J. W., Glossary of terms used in photochemistry (IUPAC Recommendations 1996). *Pure & Appl. Chem.* **1996**, *68*, 2223-2286.

56. Pinalli, R.; Pedrini, A.; Dalcanale, E., Biochemical sensing with macrocyclic receptors. *Chem. Soc. Rev.* **2018**, *47*, 7006-7026.

57. Deng, C. L.; Bard, J. P.; Lohrman, J. A.; Barker, J. E.; Zakharov, L. N.; Johnson, D. W.; Haley, M. M., Exploiting the Hydrogen Bond Donor/Acceptor Properties of PN-Heterocycles: Selective Anion Receptors for Hydrogen Sulfate. *Angew. Chem. Int. Ed.* **2019**, *58*, 3934-3938.

58. Zhao, W.; Qiao, B.; Tropp, J.; Pink, M.; Azoulay, J. D.; Flood, A. H., Linear Supramolecular Polymers Driven by Anion-Anion Dimerization of Difunctional Phosphonate Monomers Inside Cyanostar Macrocycles. *J. Am. Chem. Soc.* **2019**, *141*, 4980-4989.

59. Lee, S.; Chen, C. H.; Flood, A. H., A pentagonal cyanostar macrocycle with cyanostilbene CH donors binds anions and forms dialkylphosphate [3]rotaxanes. *Nat. Chem.* **2013**, *5*, 704-710.

60. Bricks, J. L.; Kovalchuk, A.; Trieflinger, C.; Nofz, M.; Büschel, M.; Tolmachev, A. I.; Daub, J.; Rurack, K., On the Development of Sensor Molecules that Display Fe^{III}-amplified Fluorescence. *J. Am. Chem. Soc.* **2005**, *127*, 13522– 13529.

61. Yuan, M. J. L., Y. L.; Li, J. B.; Li, C. H.; Liu, X. F.; Lv, J.; Xu, J. L.; Liu, H. B.; Wang, S.; Zhu, D. B., On the Development of Sensor Molecules that Display FeIII-amplified Fluorescence. *Org. Lett.* **2007**, *9*, 2313– 2316.

62. Pedersen, C. J., Cyclic polyethers and their complexes with metal salts. *J. Am. Chem. Soc.* **1967**, *89*, 2495-2496.

63. Pedersen, C. J., Cyclic polyethers and their complexes with metal salts. *J. Am. Chem. Soc.* **1967**, *89*, 7017-7036.

64. E. Lippert, W. L., F. Moll, W. N-gele, H. Boos, H. Prigge, I. Seibold-Blankenstein, Umwandlung von Elektronenanregungsenergie. *Angew. Chem.* **1961**, *73*, 695–706.

65. Benson, C. R.; Maffeo, C.; Fatila, E. M.; Liu, Y.; Sheetz, E. G.; Aksimentiev, A.; Singharoy, A.; Flood, A. H., Inchworm movement of two rings switching onto a thread by biased Brownian diffusion represent a three-body problem. *Proc. Natl. Acad. Sci. U.S.A.* **2018**, *115*, 9391-9396.

66. Miyaura, N. Y., K; Suzuki, A, A new stereospecific cross-coupling by the palladium-catalyzed reaction of 1-alkenylboranes with 1-alkenyl or 1-alkynyl halides. *Tet. Lett.*, *36*, 3437-3440.

67. Amar H. Flood, S. L., Kevin McDonald, Poly-Cyanostilbene Macrocycles. *US20170313652A1* **US20170313652A1**, *Nov 2, 2017*.

68. Wang, J.; Liu, K.; Ma, L.; Zhan, X., Triarylamine: Versatile Platform for Organic, Dye-Sensitized, and Perovskite Solar Cells. *Chem. Rev.* **2016**, *116*, 14675-14725.

69. Braslavsky, S. E., Glossary of terms used in photochemistry, 3rd edition (IUPAC Recommendations 2006). *Pure and Applied Chemistry* **2007**, *79*, 293-465.

70. Benniston, A. C.; Harriman, A.; Lawrie, D. J.; Mayeux, A., The photophysical properties of a pyrene–thiophene–terpyridine conjugate and of its zinc(II) and ruthenium(II) complexes. *Phys. Chem. Chem. Phys.* **2004**, *6*, 51-57.

71. Kaneda, K.; Arai, T., Photoinduced hydrogen atom transfer in trans-1-(1'-hydroxy-2'-naphthyl)-3-(1-naphthyl)-2-propen-1-one. *Photochem. Photobiol. Sci.* **2003**, *2*, 402-406.

72. Cortés, J.; Heitele, H., Band-Shape Analysis of the Charge-Transfer Fluorescence in Barrelene-Based Electron Donor-Acceptor Compounds. *J. Phys. Chem.* **1994**, *98*, 2527-2536.

73. Beens, H.; Knibbe, H.; Weller, A., Dipolar Nature of Molecular Complexes Formed in the Excited State. *J. Chem. Phys.* **1967**, *47*, 1183-1184.

74. Khalil, O. S.; Hofeldt, R. H.; McGlynn, S. P., Electronic Spectroscopy of Highly-Polar Aromatics. V. The Polar Excimer of N,N-Dialkyl-*p*-Cyanoaniline. *J. Lumin.* **1973**, *6*, 229-244.

75. Khalil, O. S.; Hofeldt, R. H.; McGlynn, S. P., Electronic Spectroscopy of Highly-Polar Aromatics. Molecular Interactions in the Ground and Excited States of N,N-Dimethyl-*p*-Cyanoaniline. *Chem. Phys. Lett.* **1972**, *17*, 479-481.

76. Khalil, O. S.; Hofeldt, R. H.; McGlynn, S. P., Electronic Spectroscopy of Highly-polar Aromatics. VI. A Self-Complex of N,N-Dialkyl-p-Cyanoanilines. *Spectrosc. Lett.* **1973**, 147-165.

77. Khalil, O. S., On the excimer model of N,N-dialkyl-p-cyanoanilines fluorescence in polar solvents. *Chem. Phys. Lett.* **1975**, *2*, 172-174.

78. Zhu, L.; Zhao, Y., Cyanostilbene-based intelligent organic optoelectronic materials. *J. Mater. Chem. C* **2013**, *1*, 1059-1065.

79. Rettig, W.; Zander, M., On Twisted Intramolecular Charge Transfer (TICT) States in N-Aryl Carbazoles. *Chem. Phys. Lett* **1982**, *87*, 229−234.

80. Taniguchi, T.; Wang, J.; Irle, S.; Yamaguchi, S., TICT fluorescence of N-borylated 2,5-diarylpyrroles: a gear like dual motion in the excited state. *Dalton Trans.* **2013**, *42*, 620-624.

81. Sasaki, S.; Niko, Y.; Klymchenko, A. S.; Konishi, G.-i., Design of donor–acceptor geometry for tuning excited-state polarization: fluorescence solvatochromism of push–pull biphenyls with various torsional restrictions on their aryl–aryl bonds. *Tetrahedron* **2014**, *70*, 7551-7559.

82. Lippert, E.; Lüder, W.; Boos, H., *Advances in Molecular Spectroscopy,* 443–457 (edited by A. Mangini). Pergamon Press, Oxford, **1962**.

83. Atsbeha, T.; Mohammed, A. M.; Redi-Abshiro, M., Excitation wavelength dependence of dual fluorescence of DMABN in polar solvents. *J. Fluoresc.* **2010**, *20*, 1241-1248.

84. Kivala, M.; Diederich, F., Acetylene-Derived Strong Organic Acceptors for Planar and Nonplanar Push−Pull Chromophores. *Acc. Chem. Res.* **2009**, *42*,235–248.

85. Matteucci, E.; Baschieri, A.; Sambri, L.; Monti, F.; Pavoni, E.; Bandini, E.; Armaroli, N., Carbazole-Terpyridine Donor-Acceptor Dyads with Rigid pi-Conjugated Bridges. *Chempluschem* **2019**, *84*, 1353-1365.

86. Lu, J.; Pattengale, B.; Liu, Q.; Yang, S.; Shi, W.; Li, S.; Huang, J.; Zhang, J., Donor-Acceptor Fluorophores for Energy-Transfer-Mediated Photocatalysis. *J. Am. Chem. Soc.* **2018**, *140*, 13719-13725.

87. Liu, Y.; Singharoy, A.; Mayne, C. G.; Sengupta, A.; Raghavachari, K.; Schulten, K.; Flood, A. H., Flexibility Coexists with Shape-Persistence in Cyanostar Macrocycles. *J. Am. Chem. Soc.* **2016**, *138*, 4843-4851.

88. Phelan, B. T.; Zhang, J.; Huang, G. J.; Wu, Y. L.; Zarea, M.; Young, R. M.; Wasielewski, M. R., Quantum Coherence Enhances Electron Transfer Rates to Two Equivalent Electron Acceptors. *J. Am. Chem. Soc.* **2019**, *141*, 12236-12239.

89. Lin, J.; Balamurugan, D.; Zhang, P.; Skourtis, S. S.; Beratan, D. N., Two-Electron Transfer Pathways. *J. Phys. Chem. B* **2015**, *119*, 7589-7597.

90. Ratner, M. A., Bridge-Assisted Electron Transfer: Effective Elelctronic Coupling. *J. Phys. Chem.* **1990**, *94*, 4877-4883.

91. Beratan, D. N.; Hopfield, J. J., Calculation of Electron Tunneling Matrix Elements in Rigid Systems: Mixed-Valence Dithiaspirocyclobutane Molecules. *J. Am. Chem. Soc.* **1984**, *106*, 1584-1594.

92. Lewis, G. N.; Kasha, M., Phosphorescence and the Triplet State. *J. Am. Chem. Soc.* **1944**, *66*, 2100.

93. Balzani V., B. F., Gandolfi M.T., Maestri M., Bimolecular electron transfer reactions of the excited states of transition metal complexes. In: Organic Chemistry and Theory. *Topics in Current Chemistry* **1978**, *75*, 1.

94. Rehm, D., Kinetics of Fluorescence Quenching by Electron and H-Atom Transfer. *Isr. J. Chem.* **1970**, *8*, 259.

95. Benson, C. R.; Fatila, E. M.; Lee, S.; Marzo, M. G.; Pink, M.; Mills, M. B.; Preuss, K. E.; Flood, A. H., Extreme Stabilization and Redox Switching of Organic Anions and Radical Anions by Large-Cavity, CH Hydrogen-Bonding Cyanostar Macrocycles. *J. Am. Chem. Soc.* **2016**, *138*, 15057-15065.

96. Marcus, R. A., Relation between Charge Transfer Absorption and Fluorescence Spectra and the Inverted Region. *J. Phys. Chem.* **1989**, *93*, 3078–3086.

97. Vandewal, K.; Benduhn, J.; Nikolis, V. C., How to determine optical gaps and voltage losses in organic photovoltaic materials. *Sustain. Energy Fuels* **2018**, *2*, 538-544.

98. Vander Griend, D. A.; Bediako, D. K.; DeVries, M. J.; DeJong, N. A.; Heeringa, L. P., Detailed Spectroscopic, Thermodynamic, and Kinetic Characterization of Nickel(II) Complexes with 2,2'-Bipyridine and 1,10-Phenanthroline Attained via Equilibrium-Restricted Factor Analysis. *Inorg. Chem.* **2008**, *47*, 656-662.

99. Fatila, E. M.; Pink, M.; Twum, E. B.; Karty, J. A.; Flood, A. H., Phosphate-phosphate oligomerization drives higher order co-assemblies with stacks of cyanostar macrocycles. *Chem. Sci.* **2018**, *9*, 2863-2872.

100. Dobscha, J. R.; Debnath, S.; Fadler, R. E.; Fatila, E. M.; Pink, M.; Raghavachari, K.; Flood, A. H., Host-Host Interactions Control Self-assembly and Switching of Triple and Double Decker Stacks of Tricarbazole Macrocycles Co-assembled with anti-Electrostatic Bisulfate Dimers. *Chem. Eur. J.* **2018**, *24*, 9841-9852.

101. Sheetz, E. G.; Qiao, B.; Pink, M.; Flood, A. H., Programmed Negative Allostery with Guest-Selected Rotamers Control Anion-Anion Complexes of Stackable Macrocycles. *J. Am. Chem. Soc.* **2018**, *140*, 7773-7777.

102. Qiao, B.; Leverick, G. M.; Zhao, W.; Flood, A. H.; Johnson, J. A.; Shao-Horn, Y., Supramolecular Regulation of Anions Enhances Conductivity and Transference Number of Lithium in Liquid Electrolytes. *J. Am. Chem. Soc.* **2018**, *140*, 10932-10936.

103. Zahran, E. M.; Fatila, E. M.; Chen, C. H.; Flood, A. H.; Bachas, L. G., Cyanostar: C-H Hydrogen Bonding Neutral Carrier Scaffold for Anion-Selective Sensors. *Anal. Chem.* **2018**, *90*, 1925-1933.

104. Dobscha, J. R.; Liu, Y.; Flood, A. H., Shape-Persistent Anion Receptors. In *Comprehensive Supramolecular Chemistry II*, **2017**; pp 329-348.

105. Fatila, E. M.; Twum, E. B.; Karty, J. A.; Flood, A. H., Ion Pairing and Co-facial Stacking Drive High-Fidelity Bisulfate Assembly with Cyanostar Macrocyclic Hosts. *Chem. Eur. J.* **2017**, *23*, 10652-10662.

106. Qiao, B.; Hirsch, B. E.; Lee, S.; Pink, M.; Chen, C. H.; Laursen, B. W.; Flood, A. H., Ion-Pair Oligomerization of Chromogenic Triangulenium Cations with Cyanostar-Modified Anions That Controls Emission in Hierarchical Materials. *J. Am. Chem. Soc.* **2017**, *139*, 6226-6233.

107. Zhao, W.; Qiao, B.; Chen, C. H.; Flood, A. H., High-Fidelity Multistate Switching with Anion-Anion and Acid-Anion Dimers of Organophosphates in Cyanostar Complexes. *Angew. Chem. Int. Ed.* **2017**, *56*, 13083-13087.

108. Qiao, B.; Anderson, J. R.; Pink, M.; Flood, A. H., Size-matched recognition of large anions by cyanostar macrocycles is saved when solvent-bias is avoided. *Chem. Commun.* **2016**, *52*, 8683-8686.

109. Lee, S.; Hirsch, B. E.; Liu, Y.; Dobscha, J. R.; Burke, D. W.; Tait, S. L.; Flood, A. H., Multifunctional Tricarbazolo Triazolophane Macrocycles: One-Pot Preparation, Anion Binding, and Hierarchical Self-Organization of Multilayers. *Chem. Eur. J.* **2016**, *22*, 560-569.

110. Qiao, B.; Liu, Y.; Lee, S.; Pink, M.; Flood, A. H., A high-yield synthesis and acid-base response of phosphate-templated [3]rotaxanes. *Chem. Commun.* **2016**, *52*, 13675-13678.

111. Fatila, E. M.; Twum, E. B.; Sengupta, A.; Pink, M.; Karty, J. A.; Raghavachari, K.; Flood, A. H., Anions Stabilize Each Other inside Macrocyclic Hosts. *Angew. Chem. Int. Ed.* **2016**, *55*, 14057-14062.

112. Singharoy, A.; Venkatakrishnan, B.; Liu, Y.; Mayne, C. G.; Lee, S.; Chen, C. H.; Zlotnick, A.; Schulten, K.; Flood, A. H., Macromolecular Crystallography for Synthetic Abiological Molecules: Combining xMDFF and PHENIX for Structure Determination of Cyanostar Macrocycles. *J. Am. Chem. Soc.* **2015**, *137*, 8810-8818.

113. Chen, T.-H.; Lee, S.; Flood, A. H.; Miljanić, O. Š., How to print a crystal structure model in 3D. *CrystEngComm* **2014**, *16*, 5488-5493.

114. Hirsch, B. E.; Lee, S.; Qiao, B.; Chen, C. H.; McDonald, K. P.; Tait, S. L.; Flood, A. H., Anion-induced dimerization of 5-fold symmetric cyanostars in 3D crystalline solids and 2D self-assembled crystals. *Chem. Commun.* **2014**, *50*, 9827-9830.

115. McNaught, A. D.; Wilkinson, A., IUPAC Compendium of Chemical Terminology, 2nd ed. (the "Gold Book"). Blackwell Scientific Publications, Oxford: 1997.

116. Hestand, N. J.; Spano, F. C., Expanded Theory of H- and J-Molecular Aggregates: The Effects of Vibronic Coupling and Intermolecular Charge Transfer. *Chem. Rev.* **2018**, *118*, 7069-7163.

117. Ueno, Y.; Jose, J.; Loudet, A.; Perez-Bolívar, C.; Anzenbacher, P.; Burgess, K., Encapsulated Energy-Transfer Cassettes with Extremely Well Resolved Fluorescent Outputs. *J. Am. Chem. Soc.* **2011**, *133*, 51.

118. Lin, W.; Yuan, L.; Cao, Z.; Feng, Y.; Song, J., Through-bond energy transfer cassettes with minimal spectral overlap between the donor emission and acceptor absorption: coumarin-rhodamine dyads with large pseudo-Stokes shifts and emission shifts. *Angew. Chem. Int. Ed.* **2010**, *49*, 375-379.

119. Kim, T. I.; Jin, H.; Bae, J.; Kim, Y., Excimer Emission-Based Fluorescent Probe Targeting Caspase-3. *Anal. Chem.* **2017**, *89*, 10565-10569.

Table of Contents